Supporting Information

Hierarchical Structure Promoted Lithiation/Delithiation Behavior of Double-Carbon Microspheres Supported Nano-Co_3O_4 Anode

Min Liu,[†‡] Hai Li,[†] Jie Yu,[†] Shuo Zhang,[‡§] Qi Chen,[‡] Wei Lu,[‡] Anbao Yuan,[*§] Li Zhong[*†] and Litao Sun[†]

[†]SEU-FEI Nano-Pico Center, Key Laboratory of MEMS of Ministry of Education, School of Integrated Circuits, Southeast University, Nanjing 210096, China

[‡]i-Lab, CAS Center for Excellence in Nanoscience, Suzhou Institute of Nano-Tech and Nano-Bionics (SINANO), Chinese Academy of Sciences, Suzhou 215123, China

[§]Department of Chemistry, College of Sciences, Shanghai University, Shanghai 200444, China

*Corresponding author.

E-mail address: abyuan@shu.edu.cn (A. Yuan)

E-mail address: lizhong@seu.edu.cn (L. Zhong)

1. Methods

1.1 Materials preparation

Preparation of carbon nanotube–ketjen black composite microspheres (DCMS). First, 2.5 g of multiwalled carbon nanotubes (CNTs), 7.5 g of ketjen black (KBs) and 5 g of LA132 (a waterborne adhesive of acrylonitrile polymer) aqueous solution (15 wt%) were added into 900 mL of deionized water and 100 mL of ethanol, followed by ultrasonic treatment for 30 min. Then, the CNT and KB microspheres (DCMS) were obtained by spray drying of the mixture followed by heat treatment at 700 °C for 4 h in N_2 atmosphere (with a heating rate of 5 °C min^{-1}).

Preparation of carbon nanotube microspheres (CMS). First, 30 g of CNTs were added into a mixed solution of 900 mL of deionized water and 100 mL of ethanol, followed by ultrasonic treatment for 30 min. Then, the CNT microspheres (CMS) were obtained by spray drying of the mixture followed by heat treatment at 700 °C for 4 h in N_2 atmosphere (with a heating rate of 5 °C min^{-1}).

1.2 Materials Characterization

The samples were characterized by X-ray diffractionmeter (XRD, Bruker D8 ADVANCE) with Cu Ka radiation (λ = 1.54056 Å), scanning electron microscope (SEM, JEOL JM3−6390) coupled with an energy-dispersive X-ray spectrometer (EDS) for elemental analysis, high-resolution transmission electron microscope (HRTEM, FEI Tecnai G2 20), and surface area and porosity analyzer (3H−2000, Beishide Instrument Technology (Beijing) Co., Ltd) at −196 °C for low-temperature nitrogen adsorption−desorption isotherms and pore-size distribution analysis.

Thermogravimetric analysis was performed on Pyris 1 TGA (Perkin Elmer) within the temperature range of 25–800 °C at a heating rate of 10 °C min^{-1} under static air atmosphere.

1.3 Electrochemical Measurements

Electrochemical performances of the active materials (bare Co_3O_4, Co_3O_4/CMS and Co_3O_4/DCMS) were investigated using coin-type cells (CR 2025). Each working electrode was prepared through a slurry-coating process, where the slurry consisting of active material (80 wt%), acetylene black (10 wt%) and polyvinylidene fluoride (PVDF, 10 wt%) dissolved in N-methyl pyrrolidone (NMP) was coated onto the copper foil current collector with an active material loading of ca. 1.3 mg cm^{-2}. The coin-type cell was assembled in an argon-filled glove box, consisting of a working electrode, a lithium counter electrode and a lithium reference electrode. The electrolyte consists of 1 M $LiPF_6$ dissolved in ethylene carbonate (EC), ethyl methyl carbonate (EMC) and dimethyl carbonate (DMC) (1:1:1, in volume), and the separator is the polypropylene micro-porous film (Cellgard 2400).

Cyclic voltammetry (CV) measurements were conducted using a CHI 600E electrochemical working station at a scan rate of 0.2 mV s^{-1} over the potential range of 0.01−3 V (vs. Li^+/Li). Electrochemical impedance spectroscopy (EIS) measurements were performed using the same apparatus in the frequency range from 100 kHz to 10 mHz. Galvanostatic discharge/charge tests were carried out on Neware CT−3008−S4 battery cycler (China) in the potential range of 0.01−3 V (vs. Li^+/Li). All measurements were conducted at room temperature. In this paper, for each electrode, the electrochemical data such as current density and specific capacity are calculated based on the mass of active material (e.g. Co_3O_4/DCMS) in the electrode.

1.4 In situ TEM experiments

In-situ TEM experiments were conducted using a PicoFemto TEM holder. The sample electrode (Co_3O_4, Co_3O_4/CMS and Co_3O_4/DCMS) was attached to one tip of a 0.3 mm-thick gold (Au) rod. Then a small amount of lithium (Li) metal was scratched onto a sharp tungsten (W) tip, serving as the counter Li electrode and Li source. Both the sample and Li electrodes were mounted onto the PicoFemto holder and quickly transferred into the TEM column. During the charge transfer process, a native Li_2O layer was formed on the surface of the Li metal, serving as the solid-state electrolyte for lithium ion transport. The Li_2O/Li and Co_3O_4/DCMS electrodes were brought into contact by the piezo-manipulator of the TEM holder. Once the contact was established, a -2 V/3 V potential was applied to the sample electrode against the Li counter electrode.

2. Estimation of volume changes

During in-situ TEM observation, the images provide geometrical information on a 2-D level. As a result, the volume expansion is derived by monitoring the evolutions in the projected area of an interested sample region. In Fig. 6b for example, a target region of the Co_3O_4/DCMS sample is outlined in cyan, which is representative of the

Co_3O_4/DCMS hierarchical structure featured by numerous Co_3O_4 nanoparticles dispersed in a porous DCMS framework. Although individual single-crystalline Co_3O_4 nanoparticles tend to undergo anisotropic volume expansion during lithium incorporation, the random orientation of nanoparticles contained in an ensemble averaged out such anisotropy, resulting in isotropic overall volume expansion of the ensemble when it consists of a large number of nanoparticles, e.g. the case in Fig. 6b. As such the 3-D volume changes of a target region can be estimated based on changes in the 2-D projected area according to the following relationship:

$$B = (A + 1)^{\frac{3}{2}}$$

A: Percentage increase in area; B: Percentage increase in volume.

The area of the target region in Fig. 6b is measured an increase of 14% after lithiation (Fig. 6d), resulting in an approximately 21% volume expansion (Fig. 6l).

3. Electrochemical properties of Co_3O_4/DCMS and Co_3O_4/CMS samples with the same carbon material content added.

Since CMS and DCMS have different pore structures and specific surface areas, the effective amount of $Co(NO_3)_2 \cdot 6H_2O$ solution uptake in the experimental preparation is different. The properties of Co_3O_4/CMS and Co_3O_4/DCMS complexes prepared with the same feed ratios were compared in the main text of the original article, and the percentages of Co_3O_4 in the two complexes were 74.6% and 57.1%, respectively. In order to further compare the electrochemical performance of Co_3O_4/DCMS and Co_3O_4/CMS samples with the same carbon material content, the input amount of

$Co(NO_3)_2 \cdot 6H_2O$ solution was reduced during the preparation of Co_3O_4/CMS samples, and Co_3O_4/CMS samples containing 59.9% Co_3O_4 were finally obtained.

The method for preparing Co_3O_4/CMS is as follows: First, 4.4 g of $Co(NO_3)_2 \cdot 6H_2O$ (Aladdin) was dissolved in 10 mL of deionized water and 10 mL of glycol, and stirred for 30 min. Then 1.00 g of CMS were added into the mixed solvent and stirred for 30 min. The resulting suspension was transferred into an autoclave and kept at 160 °C for 24 h in a drying box. Thereafter, the resulting mixture was centrifuged for 10 min at 8000 rpm, and the precipitate was washed by deionized water and ethanol successively for three times. The isolated precipitate was dried and then heat treated in an oven at 300 °C in air for 6 h. After cooling down naturally to ambient temperature.

As can be seen in Figure S3, By adjusting the amount of $Co(NO_3)_2 \cdot 6H_2O$ solution added to the CMS. The carbon content of both Co_3O_4/DCMS and Co_3O_4/CMS electrodes were determined to be close to 40%. The electrochemical properties of Co_3O_4/DCMS and Co_3O_4/CMS samples with the same carbon material content added were also compared.

4. In situ observation of the lithiation of Co_3O_4/CMS

As shown in Figure 2h, Co_3O_4/CMS consists of both supported and unsupported Co_3O_4 nanoparticles (in the form of nanowire bundles). The (de)lithiation behavior of Co_3O_4/CMS thus appears as a combination of those of Co_3O_4 (i.e., unsupported Co_3O_4 nanowire bundles) and Co_3O_4/DCMS (i.e., well-supported Co_3O_4 particles), as corroborated by both ex-situ TEM characterization (Fig. 5d-f) and in-situ TEM study (Figure S7). The unsupported Co_3O_4 nanowire bundles in Co_3O_4/CMS lead to significant structural swelling and degradation during lithiation (Figure S7g-l). As a result, such a mixed (de)lithiation behavior leads to mediocre cyclability in the Co_3O_4/CMS electrode (Fig. 5c).

5. Supplementary figures and tables

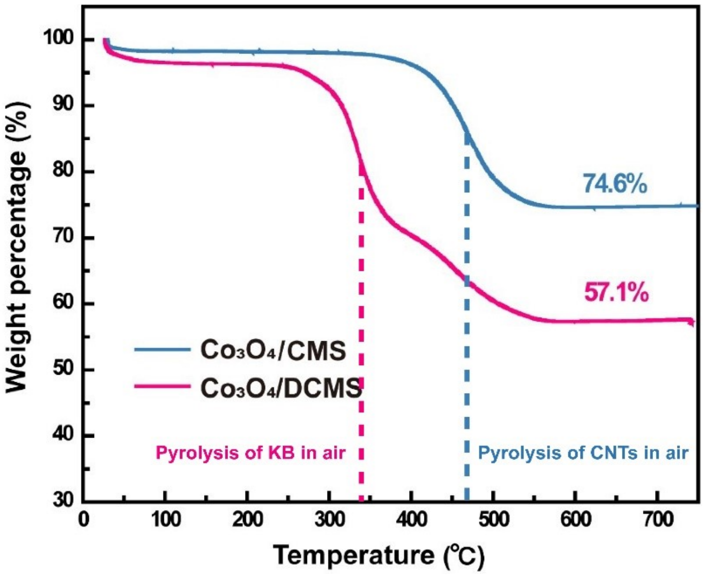

Figure S1. TG curves of Co_3O_4/CMS and Co_3O_4/DCMS composites.

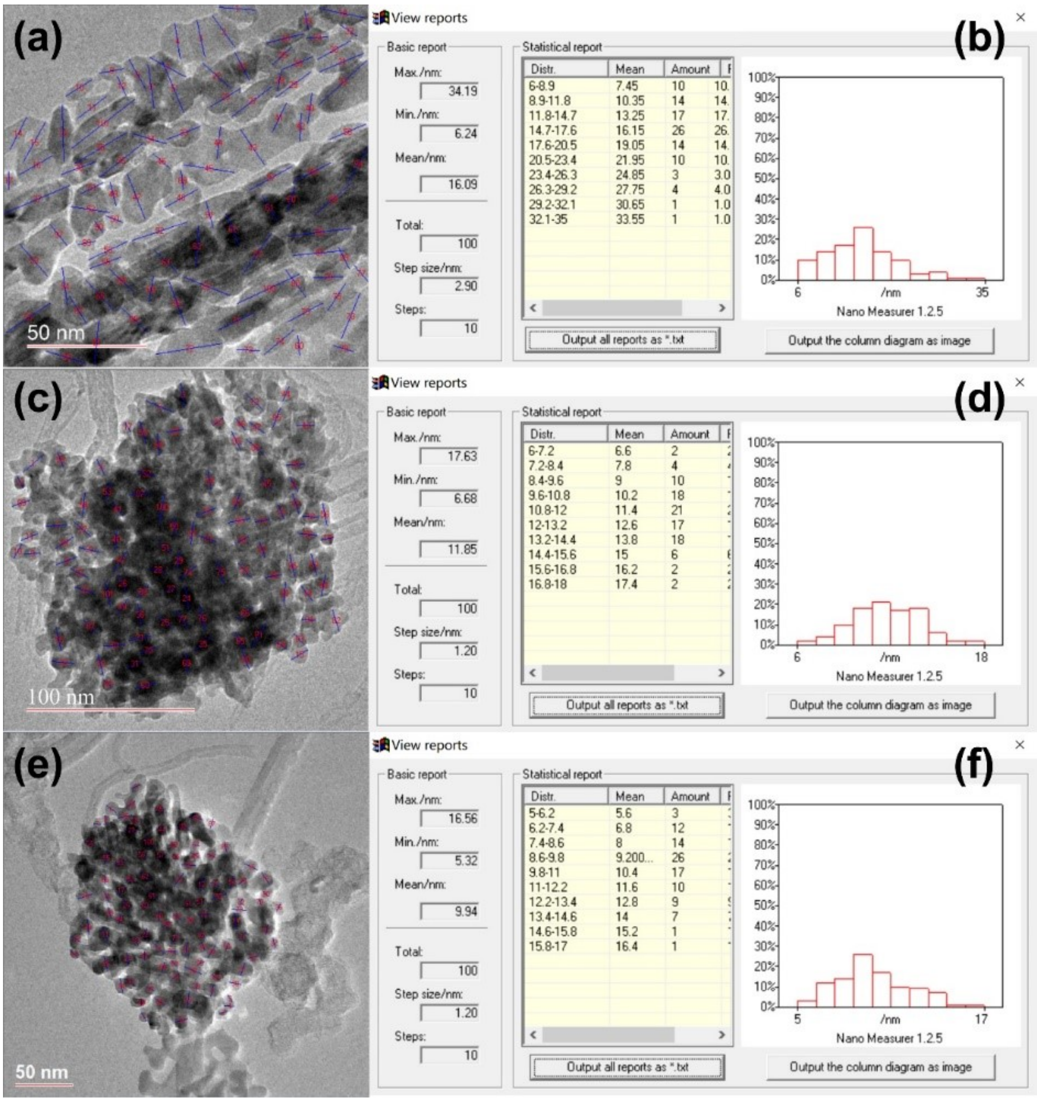

(b)

Basic report

Max./nm: 34.19

Min./nm: 6.24

Mean/nm: 16.09

Total: 100

Step size/nm: 2.90

Steps: 10

Statistical report

Distr.	Mean	Amount	F
6-8.9	7.45	10	10.
8.9-11.8	10.35	14	14.
11.8-14.7	13.25	17	17.
14.7-17.6	16.15	26	26.
17.6-20.5	19.05	14	14.
20.5-23.4	21.95	10	10.
23.4-26.3	24.85	3	3.0
26.3-29.2	27.75	4	4.0
29.2-32.1	30.65	1	1.0
32.1-35	33.55	1	1.0

(d)

Basic report

Max./nm: 17.63

Min./nm: 6.68

Mean/nm: 11.85

Total: 100

Step size/nm: 1.20

Steps: 10

Statistical report

Distr.	Mean	Amount
6-7.2	6.6	2
7.2-8.4	7.8	4
8.4-9.6	9	10
9.6-10.8	10.2	18
10.8-12	11.4	21
12-13.2	12.6	17
13.2-14.4	13.8	18
14.4-15.6	15	6
15.6-16.8	16.2	2
16.8-18	17.4	2

(f)

Basic report

Max./nm: 16.56

Min./nm: 5.32

Mean/nm: 9.94

Total: 100

Step size/nm: 1.20

Steps: 10

Statistical report

Distr.	Mean	Amount
5-6.2	5.6	3
6.2-7.4	6.8	12
7.4-8.6	8	14
8.6-9.8	9.200...	26
9.8-11	10.4	17
11-12.2	11.6	10
12.2-13.4	12.8	9
13.4-14.6	14	7
14.6-15.8	15.2	1
15.8-17	16.4	1

Figure S2. (a, b) show the size distribution of Co_3O_4 nanoparticles of Co_3O_4 sample. (c, d) show the size distribution of Co_3O_4 nanoparticles of Co_3O_4/CMS sample. (e, f) show the size distribution of Co_3O_4 nanoparticles of Co_3O_4/DCMS sample.

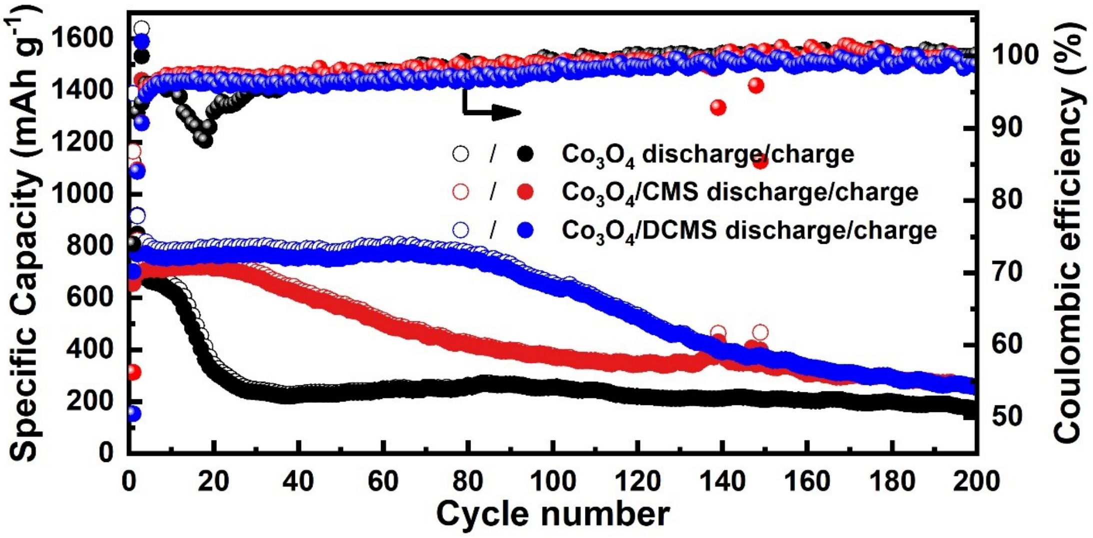

Figure S3. Cycling performances (at 300 mA g^{-1}) of Co_3O_4, Co_3O_4/CMS and Co_3O_4/DCMS electrodes within a potential window of 0.01–3 V (vs. Li^+/Li).

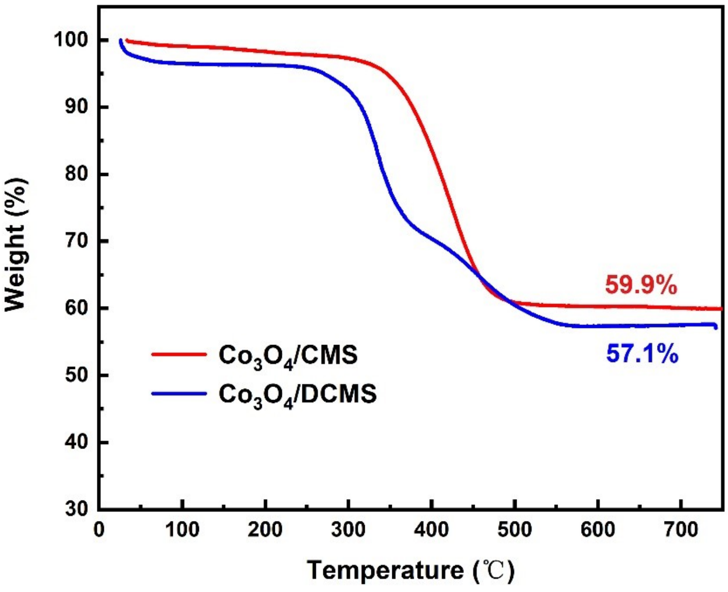

Figure S4. TG curves of Co_3O_4/CMS (the input amount of $Co(NO_3)_2 \cdot 6H_2O$ solution was reduced during the preparation) and Co_3O_4/DCMS composites.

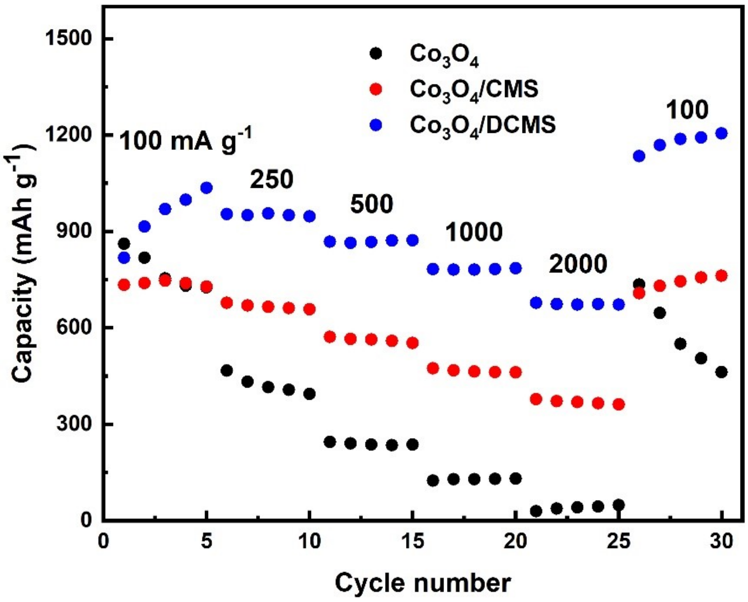

Figure S5. Rate performances of Co_3O_4, Co_3O_4/CMS and Co_3O_4/DCMS electrodes within a potential window of 0.01–3 V (vs. Li^+/Li), (57.1% and 59.9% Co_3O_4 in Co_3O_4/CMS and Co_3O_4/DCMS complexes, respectively).

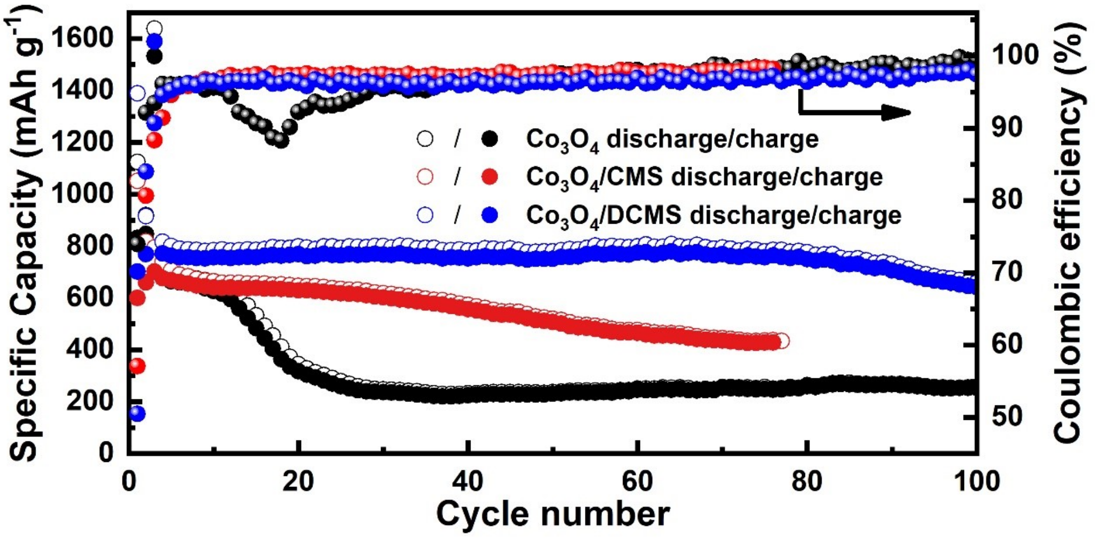

Figure S6. Cycling performances (at 300 mA g^{-1}) of Co_3O_4, Co_3O_4/CMS and Co_3O_4/DCMS electrodes within a potential window of 0.01–3 V (vs. Li^+/Li), (57.1% and 59.9% Co_3O_4 in Co_3O_4/CMS and Co_3O_4/DCMS complexes, respectively).

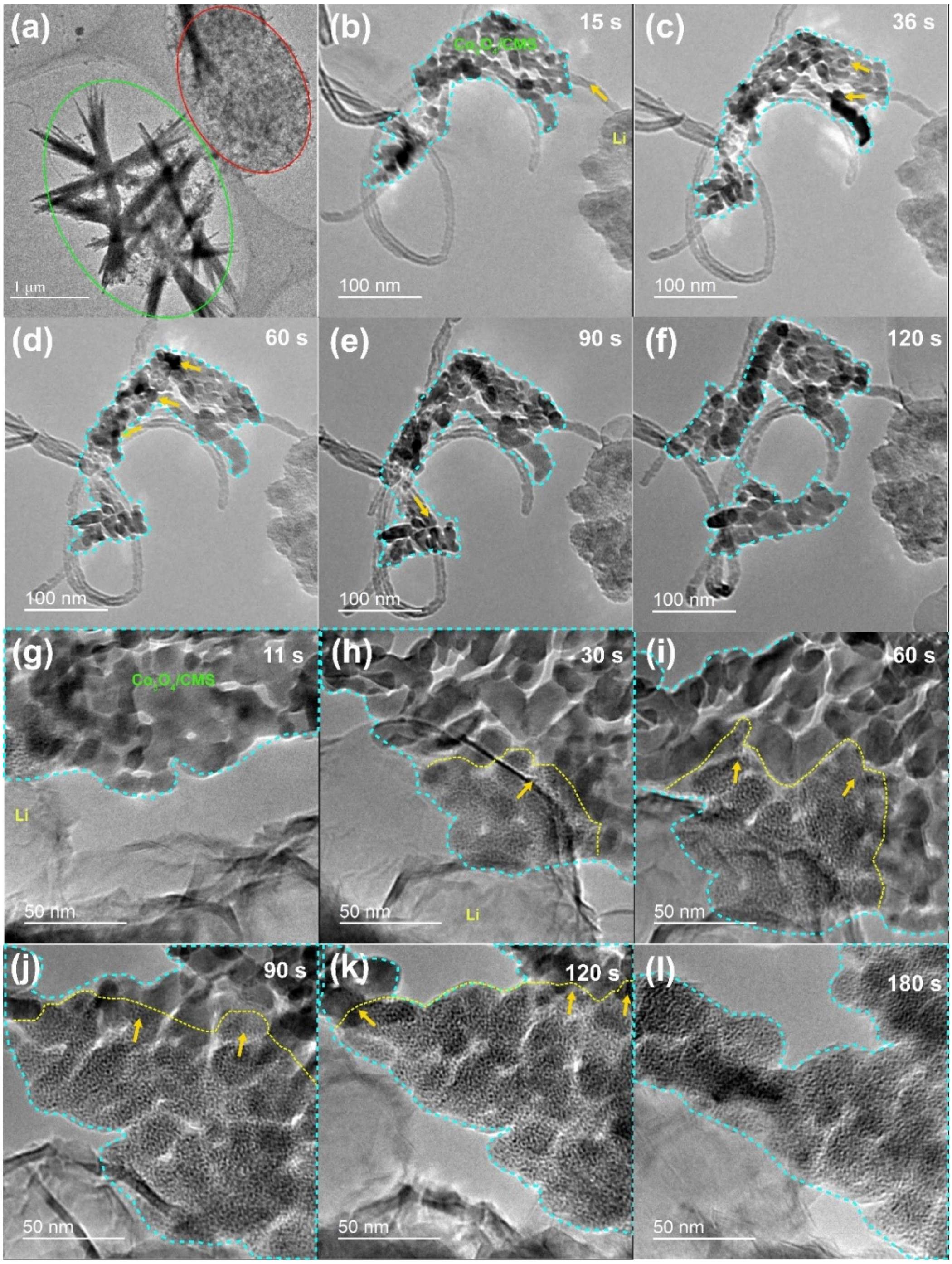

Figure S7. Time-sequence TEM images of the lithiation process of Co_3O_4/CMS at a bias of -2V with respect to Li. As shown in (a) (see also Fig. 2h), Co_3O_4/CMS consists of both supported (circled in red) and unsupported (circled in green) Co_3O_4 nanoparticles. Lithiation of CMS-supported Co_3O_4 nanoparticles (outlined by a cyan contour in b–f) demonstrate behaviors similar to Co_3O_4/DCMS (Fig. 6b-d), which is accompanied by a limited overall volume expansion of ~36%. By contrast, lithiation of unsupported Co_3O_4 nanoparticles in Co_3O_4/CMS (g–l) exhibits behaviors similar to pure Co_3O_4 featured by a severe volume expansion of ~203%. The lithiation directions are indicated by yellow arrows. The lithiation front is indicated by a yellow dashed curve.

Table S1. Charge specific capacities (in mAh g^{-1}) and coulombic efficiencies of Co_3O_4, Co_3O_4/CMS and Co_3O_4/DCMS electrodes for the first three cycles.

Sample	1st cycle	2nd cycle	3rd cycle
Co_3O_4	904.4/71.3%	820.7/82.9%	766.1/87.5%
Co_3O_4/CMS	764.9/52.6%	770.4/88.8%	787.7/91.9%
Co_3O_4/DCMS	802.7/49.6%	828.5/87.8%	862.0/92.3%

6. Supplementary movie captions

Movie S1. In-situ TEM observations showing the structural evolution of a Co_3O_4/DCMS particle during lithiation process (at a bias of -2 V applied). The movie covers a timespan of ~ 400 s.

Movie S2. In-situ TEM observations showing the structural evolution of a Co_3O_4/DCMS particle during delithiation process (at a bias of 3 V applied). The movie covers a timespan of ~ 400 s.

Movie S3. In-situ TEM observations showing the structural evolution of a Co_3O_4 particle during lithiation process of (at a bias of -2 V applied). The movie covers a timespan of ~ 400 s.

Movie S4. In-situ TEM observations showing the structural evolution of a Co_3O_4 particle during delithiation process (at a bias of 3 V applied). The movie covers a timespan of ~ 400 s.